Chapter 11
Intravital Microscopy of the Lung

Robert G. Presson, Irina Petrache, and Mary Beth Brown

Abstract Real time high quality imaging of intra-thoracic organs with sufficient resolution to study microcirculatory dynamics, inflammatory cell trafficking, and cellular and subcellular events during physiologic circulatory and breathing conditions remains a high priority in pulmonary and cardiovascular research. Recent technological developments especially in the area of two-photonmicroscopy (TPM) offer enhanced resolution and deeper penetration under the organ surface, thus allowing sampling of areas of interest to biologists and physiologists. Furthermore, with TPM one can image sub-cellular and molecular events in real time, such as protein trafficking, enzyme activation, and reactive oxygen species generation, which are pertinent to the pathogenesis of many diseases of interest to the research community. The application of TPM to organs in the thoracic cavity, and especially the lung has been hampered by cardiorespiratory motion and new techniques to mitigate these limitations have been developed. In this chapter, we will describe intravital imaging techniques applied to the lung through a historical perspective, and highlight several recent practical applications of these approaches.

Keywords Microscopy • Lung • Pulmonary • Real time • Microcirculation

Abbreviations

TPM	Two Photon microscopy
FITC	Fluorescein Isothiocyanate
PMN	Polymorphonuclear cell

This work was supported by the NIH R01HL077328 (IP)

R.G. Presson, MD (✉)
Department of Anesthesia, Indiana University,
1102 South Drive, Fessler Hall 204, Indianapolis, IN 46202, USA
e-mail: rpresson@iupui.edu

I. Petrache
Department of Medicine, Indiana University, Indianapolis, IN, USA

Richard L. Roudebush Veteran Affairs Medical Center, Indianapolis, IN, USA

M.B. Brown
Department of Physical Therapy, Indiana University, Indianapolis, IN, USA

R. Weigert (ed.), *Advances in Intravital Microscopy: From Basic to Clinical Research*, DOI 10.1007/978-94-017-9361-2_11

11.1 Techniques

The oldest technique for studying the pulmonary microcirculation and one of the most direct is intravital microscopy. This technique was first applied to the lung in 1661, when Marcello Malpighi transilluminated the frog lung with candlelight and used a microscope to observe erythrocytes moving through the pulmonary capillaries. This discovery completed the picture of the circulation developed by William Harvey through a series of experiments demonstrating that there had to be a direct connection between the venous and arterial systems throughout the body.

11.1.1 Unrestrained Motion

Since the seventeenth century, the essentials of intravital lung microscopy have remained the same as has the principal obstacle, respiratory motion. Early investigators either observed the lung without restraining respiratory motion, or suspended respiration and observed the lung in apnea. The tradeoffs of these techniques are illustrated by the classical study of (Wearn et al. 1934). These investigators dissected the chest wall of the cat down to the pleura, and transilluminated the lower edge of the lung with a quartz rod that was passed through an abdominal incision. Initial experiments were performed while the animals were breathing, and morphine was used to decrease the respiratory rate. Although these investigators reported that the difficulty of observing the moving lung grew less as their eyes became accustomed to the motion, they did not feel secure in detecting the finer capillary changes.

11.1.2 Apnea

Subsequent studies were performed animals were studied who were immobilized by the use of curare. Oxygen was insufflated into the trachea, which helped to prevent hypoxemia, but not hypercarbia and acidosis. Using this technique, Wearn made the important observation that pulmonary capillaries were intermittently perfused suggesting the possibility of a recruitable reserve. Although the experimental conditions in the first group were the most physiologic, respiratory motion interfered with the observations. In contrast, the ability to observe the microcirculation in the paralyzed animals was ideal but the observations were unavoidably affected by alterations in blood gases.

11.1.3 Vacuum Manifold

A significant advance in dealing with respiratory motion was made approximately 30 years later by Wagner who developed an implantable window that was encircled by a vacuum manifold (Wagner 1969). Gentle radial traction from the manifold

arrested cardiorespiratory motion in the observation field permitting serial measurements on the same microvascular networks without the need to alter ventilation. Using this device, Wagner et al. directly observed capillary recruitment in the dog lung when pulmonary artery pressure was raised by airway hypoxia, the first direct observation of capillary recruitment in an intact living animal.

Although the vacuum manifold effectively limited respiratory motion, itconfined observations to a small area of the subpleural microcirculation. In addition, investigators had limited control of hemodynamics in the intact animal. The geometry of the implanted manifold also imposed limitations on the characteristics of the microscope objective. The diameter of the objective either had to be small enough to fit inside the walls of the frame or the working distance had to be long enough to focus on the lung without lowering the objective into the frame. This problem was most notable with large diameter, high NA objectives with short working distances and with windows developed for implantation in smaller species such as the rat that limited the dimensions of the frames (Fig. 11.1).

One solution to this problem is to couple the lung to a vacuum manifold that is not implanted in the closed chest wall. Because manifolds used for this preparation do not need to accommodate the thickness of the chest wall they are flat across the top and therefore can accommodate objectives of any diameter or working distance (Fig. 11.2). In this preparation a thoracotomy is performed and the ribs are retracted to expose the lung. The manifold is then lowered until it contacts the pleural surface (Fig. 11.3). Although respiratory motion is greatly reduced when the manifold is coupled to the lung by vacuum, there is typically more motion than that seen in the closed thorax preparation. Alternatively windows developed for use in smaller species may lack a means of arresting cardiorespiratory motion . In this case, observations must be made during respiration or apnea as discussed above.

11.1.4 Isolated Lung

To address several of the above-mentioned problems, the isolated pump-perfused lung preparation was developed. In a typical preparation (Fig. 11.4), the main pulmonary artery is cannulated via the right ventricular outflow tract and the left atrium is cannulated via the left ventricle in small species or via the left atrial appendage in larger species. Perfusate (buffer, autologous blood, or a mixture) is pumped into the pulmonary artery with a peristaltic pump and drains passively from the left atrium into atemperature-controlledreservoir. Because the isolated lung has a relatively low metabolic rate and is not attached to a metabolically active animal, CO_2 production is minimal and due to a lack of O_2 consumption, there is essentially no alveolar-arterial O_2 gradient. Thus ventilation with a 6 % CO_2-17 % O_2-77 % N_2 gas mixture produces normal arterial blood gas tensions. The lack of metabolic activity also means that ventilation can be suspended for long periods without a significant change in blood gases. In this preparation fine control of arterial pressure, venous pressure and cardiac output can be achieved by changes in perfusion pump flow rate and venous reservoir height. The entire surface area of the lung is also available for observation.

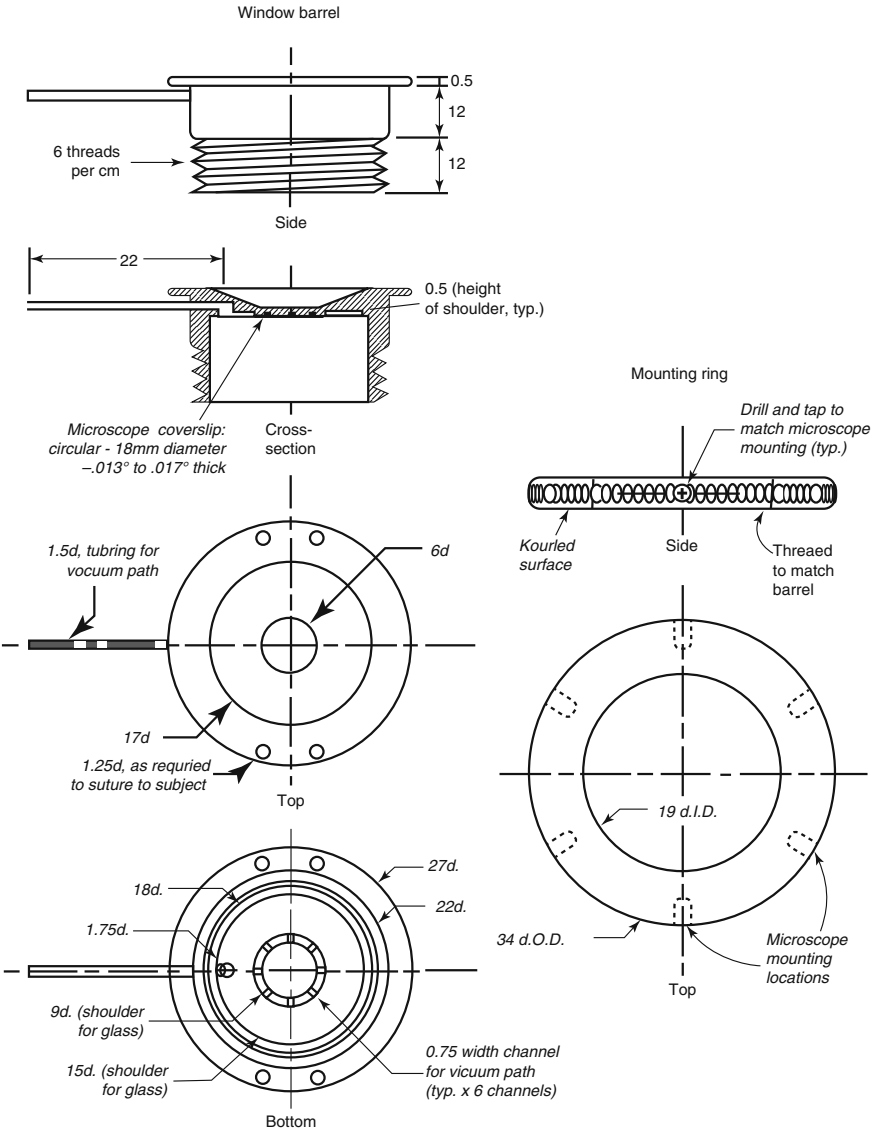

Fig. 11.1 Window for implantation in the rat

Unrestricted access to the great vessels allows for some unique techniques such as the one developed by Bhattacharya and colleagues. A microcatheter (e.g. PE-10) is passed retrograde through a pulmonary vein until it wedges in a small pulmonary vein blocking blood flow to this area. A fluorescent probe is then infused through the catheter to load the microcirculation drained by the vein. After several minutes the catheter is withdrawn and the area is reperfused removing intravascular indicator.

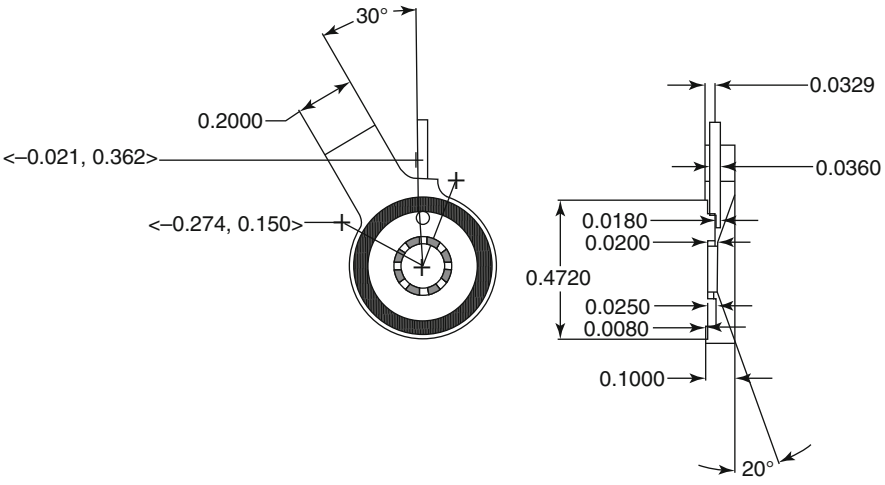

Fig. 11.2 Manifold for mouse lung

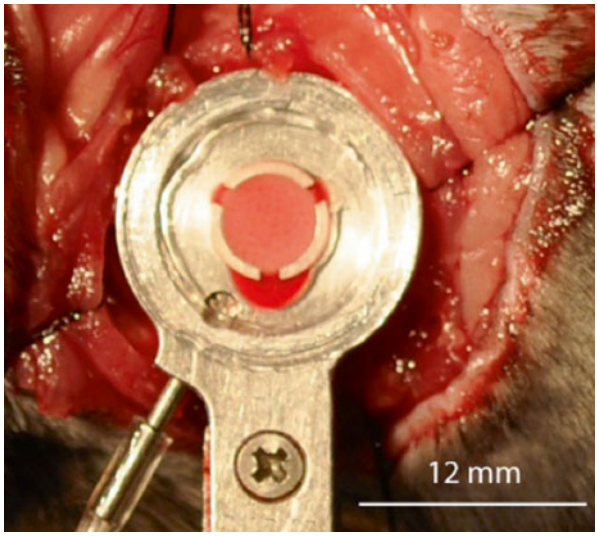

Fig. 11.3 Lung coupled to window in open mouse thorax

This technique allows loading of a small area of the microvascular endothelium with probe while avoiding significant background levels of circulating indicator.

In spite of its advantages, measurements obtained from the isolated lung vary from the intact animal (closed thorax, lungs perfused by the beating heart) for a number of reasons. First, it is commonly observed that vascular resistance is higher in the pump-perfused lung preparation. Because the distribution of resistance across the pulmonary circulation in the pump-perfused lung is similar to that in the intact animal, microvascular pressure will be higher in the pump-perfused lung resulting in a higher level of recruitment for a given flow rate.

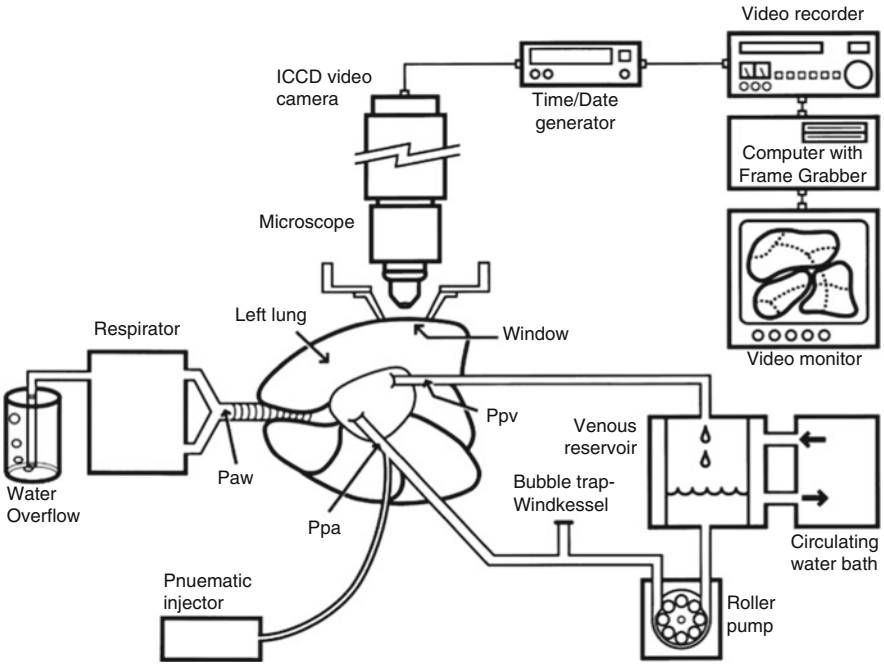

Fig. 11.4 Pump perfused lung preparation for intravital microscopy

A second problem with the pump-perfused lung arises from exposure of the perfusate to the pump circuit. It is known that complement is activated by both the classical and alternate pathways when heparinized blood is recirculated through an extracorporeal perfusion circuit. Activated complement in turn causes neutrophil activation and sequestration in the pulmonary capillaries. This is a particular problem with studies of neutrophil trafficking in the pulmonary microcirculation. Inflammatory mediators may also alter vascular tone in the vessels supplying and draining the capillary bed.

Because the level of capillary recruitment is highly dependent on the degree of alveolar wall tension, studies of microvascular perfusion may differ between the isolated lung and the intact animal. When alveolar diameters are small and wall tension is low, capillaries begin to open at a low pressure. Recruitment then proceeds rapidly such that all capillaries open with only a small increase in pressure. Under these circumstances, recruitment has been described as sheet-like. A different pattern is observed when alveolar diameter is large and wall tension is high. In this case, recruitment occurs gradually, a segment at a time, over a broad range of pressure. Which of these patterns is observed in the excised lung is dependent on the degree of lung inflation. However, it can be difficult to know how much to adjust inflating pressure to achieve a lung volume equal to that in the closed thorax. Unlike the excised lung, there is a gradient of alveolar size in the lung suspended by negative pleural pressure in the closed chest with the alveoli at the top pulled open by the weight of the lung while those at the bottom are compressed.

The isolated lung is most commonly perfused with a peristaltic pump that produces steady flow. However the lung in the intact animal is perfused with pulsatile flow. In contrast to steady flow, it has been shown that capillary recruitment is nearly double during pulsatile flow. The accompanying increase in the cross sectional area of the capillary bed may explain in part why resistance is lower in the intact lung. Taken together, these observations provide an explanation why previously reported values of microvascular gas exchange reserve in the pump-perfused lung may differ from the intact animal.

11.1.5 Gating and Frame Registration

In cases where respiratory and cardiac-induced lung motion is not eliminated by a vacuum manifold, ventilation can be synchronized with image acquisition or gated. In this case ventilation is suspended briefly while an image is acquired (1–2 s). Imaging is then paused and ventilation is resumed for a set number of breaths. This cycle then repeats until imaging is complete. Due to a lower frequency of image acquisition, gating inherently decreases temporal resolution. Alternatively motion artifact can be removed in some cases by post acquisition-processing or frame registration. Briefly, pixels are shifted in sequential images to bring them into registration thus eliminating motion (Fig. 11.5).

11.2 Major Areas of Investigation

11.2.1 Gas Exchange Reserve

The microcirculation of the normal lung has significant gas exchange reserve capacity in three forms: capillary recruitment, capillary distension, and transit time reserve. The first of these, recruitment, exists in the form of capillaries that are not perfused with red blood cells at rest, or even during moderate exercise. As oxygen demand increases, cardiac output and capillary transmural pressure rise causing recruitable capillaries to become perfused. These newly recruited capillaries directly in-crease gas exchange surface area. Increased capillary transmural pressure also causes distension of recruited capillaries, the second form of reserve, which increases the number of red blood cells in the gas exchange vessels. The third form of reserve, surplus capillary length, occurs because under basal conditions red blood cells become saturated with oxygen after crossing the first third of the capillary bed. The remaining two thirds of capillary length are utilized when red blood cell velocity increases, forcing the cells to move farther across the capillaries before they are completely saturated. This form of reserve is limited by the rate of diffusion of oxygen from alveolar gas to the hemoglobin in red blood cells. If transit times

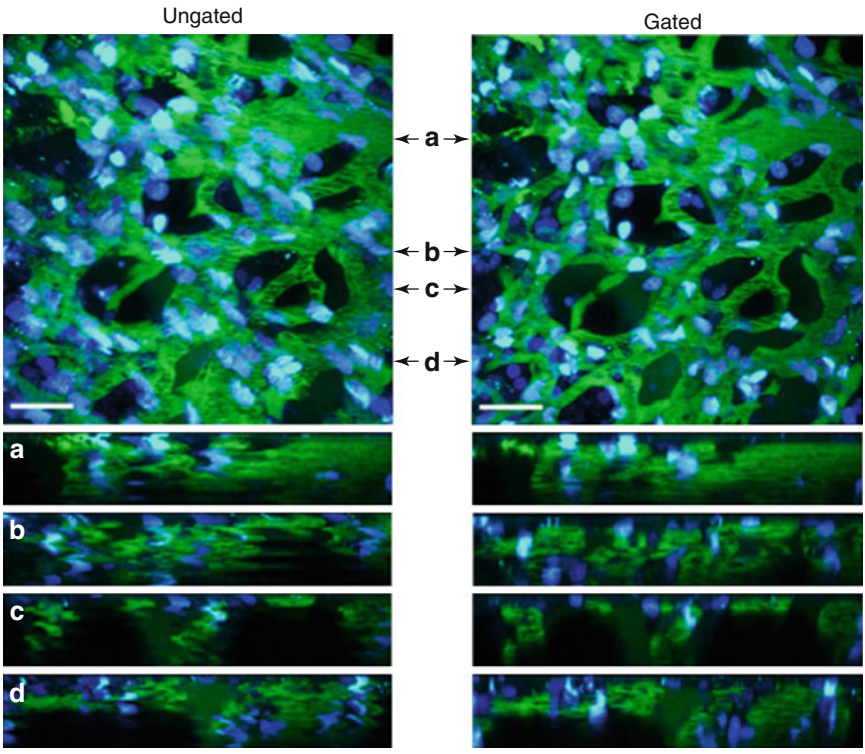

Fig. 11.5 Gated imaging eliminates motion for maximum clarity in 3-dimensional TPM reconstructions. Comparison between non-gated (**a**) and gated (**b**) image acquisition of an identical field of view showing FITC-labeled (*green*) alveolar microvasculature in the intact rat. Reconstructions in the x-z orientation correspond to the indicated slice regions (**c**, **d**) from the 3-dimensional images. Nuclei are stained with intravenously-administered Hoechst 33258 dye (blue). Scale bars = 25 μm (Reproduced from (Presson et al. 2011) with permission)

become too short (~<0.25 s under normal conditions), red blood cells may exit the capillary bed incompletely saturated. However, changes in capillary transit time are linked to the degree of recruitment and distension through their effect on capillary volume. For a given pulmonary blood flow, capillary transit time increases as capillary volume increases. In this way, recruitment and distension limit the fall in capillary transit times. Further, the transit time distribution becomes more homogeneous as pressure and flow increase with the longest transit times decreasing more than the shorter ones. This effect is presumably the result of more homogeneous recruitment and distension of pulmonary capillaries. Together these two effects help to prevent incompletely saturated red blood cells from exiting the pulmonary circulation.

The important relationships between these three forms of reserve capacity have been investigated in various species using a number of techniques. However because of technical limitations, measurement of microvascular reserve in the rat has generally

been limited to isolated pump perfused preparations or fixed tissue which may not accurately reflect reserve capacity in the intact animal (closed thorax, lungs perfused by the beating heart) for a number of reasons. For example, vascular resistance is typically increased in the isolated lung which may in turn effect capillary transmural pressure and thus the degree of recruitment and distension. Further, lung volume in the isolated lung, which has an important influence on microcirculatory perfusion through its effect on alveolar wall tension, may vary from the lung suspended in the closed thorax. Therefore actual values for pulmonary micro-vascular reserve in the intact rat remain uncertain. This is an important gap because a number of models of lung pathology (e.g. emphysema, pulmonary hypertension, and lung transplantation) are based on studies in this species. To fill this gap, we have developed an intravital microscopy model of the pulmonary microcirculation in the intact rat, and reported the first measurements of pulmonary microvascular reserve using this model (Presson et al. 2011).

11.2.2 Leukocyte Trafficking

One of the most exciting applications of intravital lung microscopy in the intact animal is the opportunity to study leukocyte trafficking. This achievement is due to elimination of leukocyte activation typically initiated by contact with foreign surfaces in the isolated pump perfused lung preparations. Therefore, leukocyte trafficking as a marker of both PMN and pulmonary endothelial cell activation during inflammation can be measured by quantifying leukocyte adhesion, rolling, and extravasation from the microcirculation into alveolar spaces. To determine leukocyte trafficking using TPM, leukocytes can be labeled either with intravenous rhodamine 6G for fluorescence imaging, or via transgenic expression of fluorescence proteins under cell-specific promoters (Fig. 11.6).

11.2.3 Vascular Permeability

Changes in vascular permeability are relevant to the development of pulmonary edema, lung inflammation, and infection. Typically, measurement of increased lung vascular permeability have relied on measuring wet and dry lung weight, or the degree of extravasation of injectable dye into airways. These measurement are tedious and imprecise. The intravital monitoring of intavascularly injected dye into the alveolar spaces offers the advantages of direct observation of increased permeability of the lung microcirculation upon application of an edemagenic agonist and that of quantification of kinetics and degrees of leaked plasma (Fig. 11.6). The limitations of this technique are the relatively short observation time, which is dependent on the duration of the preparation (hours) and the small area of observation of only dozens of alveoli, which may miss heterogeneous disease distributions.

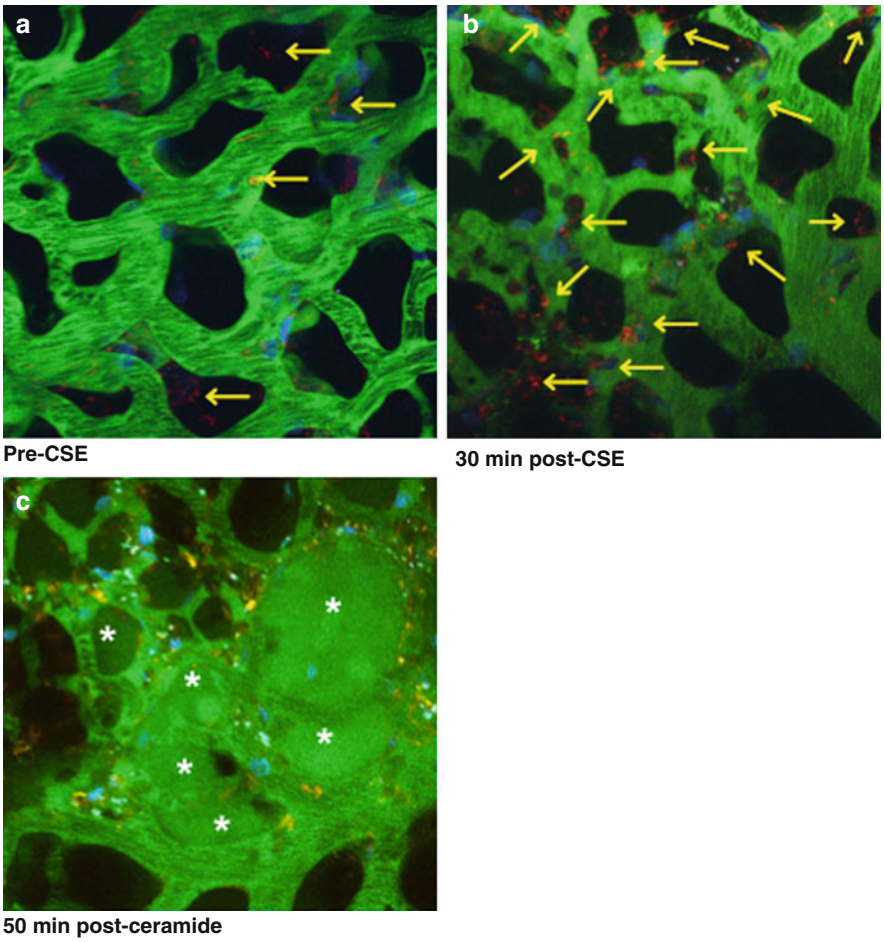

Fig. 11.6 Capturing leukocyte trafficking and plasma extravasation in real-time in the pulmonary microvasculature of a living rat. Three-dimensional reconstruction of FITC-labeled vessels (*green*) surrounding alveoli (*dark regions*) and Rho-G6-labeled neutrophils (*orange*) imaged in intravital 2-photon microscopy before (**a**) and (**b**) 30 min after intratracheally-administered cigarette smoke extract (CSE), or 50 min after intravenous administration of ceramide 16:0 PEG (**c**). Nuclei are stained with intravenously administered Hoechst 33258 dye (blue). Note increasing neutrophil trafficking (*yellow arrows*) and plasma extravasation into airspaces (*asterisks*)

11.2.4 Vasoreactivity

By injecting fluorescent plasma markers, such as labeled albumin, one can measure vascular diameters of specific vessels before and after interventions and directly gauge vascular constriction and dilation (Fig. 11.7). These measurements may be useful for screening of drug effects, as well as direct observation of ventilation perfusion relationship, for example hypoxic vasoconstriction.

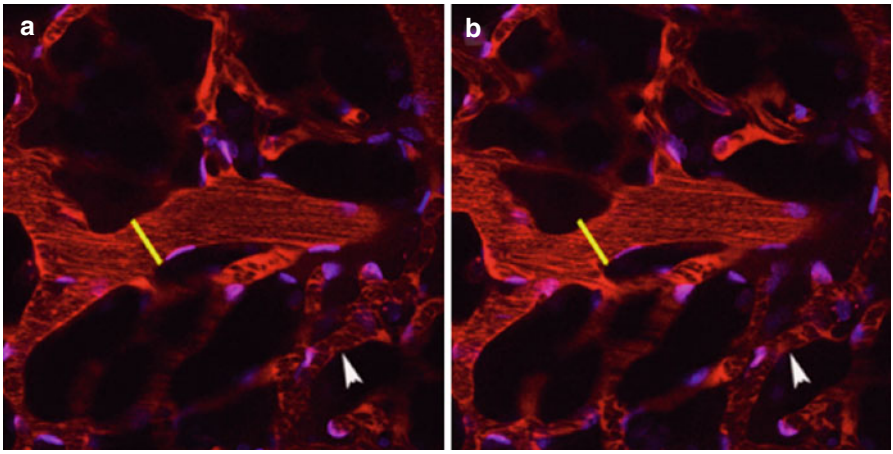

Fig. 11.7 Vasoconstriction of a TR-labeled (*red*) pulmonary arteriole in response to hypoxia (FiO_2 14 %) captured in an intact rat in real-time using 2-photon intravital microscopy during (**a**) Normoxia (**b**) Hypoxia (1 min). Note narrowing (constriction) of the pulmonary arteriole in hypoxia relative to the overlaid *yellow line*, which represents the diameter of the vessel during normoxia. Capillaries (*white arrow head*) surrounding normal alveolar airspaces (*dark*) remained unchanged in diameter during hypoxia. Nuclei are stained with intravenously administered Hoechst 33258 dye (blue) and circulating cells appear as *black streaks* within the vessels

11.2.5 Cellular Movement

Cellular movement such as migration/homing or engulfment (Megens et al. 2011),**inter-cellular connections** (Islam et al. 2012), as well as **subcellular pathology and physiology** such as structural details (e.g. endothelial glycocalyx (Yang et al. 2013)) molecular trafficking, and signal transduction are now made possible with improved resolution of microscopy and stability of lung preparations. Some of these advances have been recently reviewed (Kuebler 2011; Looney and Bhattacharya 2013). As an example, NO production and cellular localization can be distinctly visualized with TPEM, with minimal or no interference from lung autofluorescence (Fig. 11.8). Recently, inter-cellular waves of calcium signaling have been visualized using intravital lung microscopy (Westphalen et al. 2014).

In conclusion, there are exciting new developments in lung intravital microscopy which allow the visualization of previously unimagined details in the lung in real time. The cost and technical complexity of preps, the relative superficial sub pleural visualization, relatively short duration of real time monitoring, and the potential sampling error of non-homogeneous lung processes remain challenges to the widespread utilization of intravital imaging in lung research. As technology advances, it is likely these hurdles will be soon eliminated and intravital imaging in the intact animal and possibly in human lungs will become routine.

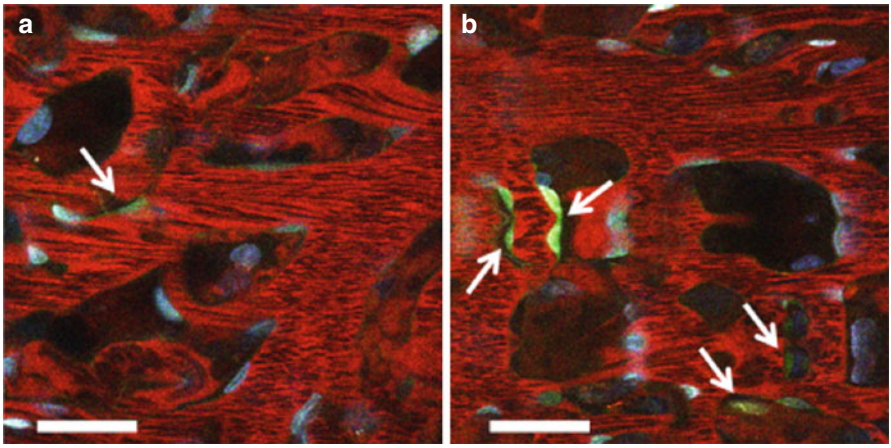

Fig. 11.8 Increase in DAF-2DA-labeled nitric oxide fluorescence (NO indicator) (*green*, *arrows*) in TR-labeled (*red*) pulmonary microvasculature in response to i.v. sodium nitroprusside (SNP). Images were captured in an intact rat in real-time using 2-photon intravital microscopy: (**a**) pre-SNP (**b**) post-SNP. Nuclei are stained with intravenously administered Hoechst 33258 dye (blue) and circulating cells appear as *black streaks* within the vessels. Scale bar = 25 um

Acknowledgements We would like to thank Wiltz Wagner Jr., PhD for his mentoring and key role in pioneering the lung intravital imaging technique.

References

Islam MN et al (2012) Mitochondrial transfer from bone-marrow-derived stromal cells to pulmonary alveoli protects against acute lung injury. Nat Med 18:759–765. doi:10.1038/nm.2736

Kuebler WM (2011) Real-time imaging assessment of pulmonary vascular responses. Proc Am Thorac Soc 8:458–465. doi:10.1513/pats.201101-005MW

Looney MR, Bhattacharya J (2013) Live imaging of the lung. Annu Rev Physiol. doi:10.1146/annurev-physiol-021113-170331

Megens RT, Kemmerich K, Pyta J, Weber C, Soehnlein O (2011) Intravital imaging of phagocyte recruitment. Thromb Haemost 105:802–810. doi:10.1160/TH10-11-0735

Presson RG Jr et al (2011) Two-photon imaging within the murine thorax without respiratory and cardiac motion artifact. Am J Pathol 179:75–82

Wagner WW Jr (1969) Pulmonary microcirculatory observations in vivo under physiological conditions. J Appl Physiol 26:375–377

Wearn JT et al (1934) The normal behavior of the pulmonary blood vessels with observations on the intermittence of the flow of blood in the arterioles and capillaries. Am J Physiol 109:236–256

Westphalen K et al (2014) Sessile alveolar macrophages communicate with alveolar epithelium to modulate immunity. Nature. doi:10.1038/nature12902

Yang Y, Yang G, Schmidt EP (2013) In vivo measurement of the mouse pulmonary endothelial surface layer. J Vis Exp 72:e50322. doi:10.3791/50322